

VIZOR: Viewpoint-Invariant Zero-Shot Scene Graph Generation for 3D Scene Reasoning

Vivek Madhavaram^{1*}Vartika Sengar^{2*}Arkadipta De^{2*†}Charu Sharma¹¹Machine Learning Lab, IIIT Hyderabad, India²Fujitsu Research India, Bangalore

vivekvardhan.m@research.iiit.ac.in, vartika.sengar@fujitsu.com, charu.sharma@iiit.ac.in

Abstract

Scene understanding and reasoning has been a fundamental problem in 3D computer vision, requiring models to identify objects, their properties, and spatial or comparative relationships among the objects. Existing approaches enable this by creating scene graphs using multiple inputs such as 2D images, depth maps, object labels, and annotated relationships from specific reference view. However, these methods often struggle with generalization and produce inaccurate spatial relationships like “left/right”, which become inconsistent across different viewpoints. To address these limitations, we propose Viewpoint-Invariant Zero-shot scene graph generation for 3D scene Reasoning (VIZOR). VIZOR is a training-free, end-to-end framework that constructs dense, viewpoint-invariant 3D scene graphs directly from raw 3D scenes. The generated scene graph is unambiguous, as spatial relationships are defined relative to each object’s front-facing direction, making them consistent regardless of the reference view. Furthermore, it infers open-vocabulary relationships that describe spatial and proximity relationships among scene objects without requiring annotated training data. We conduct extensive quantitative and qualitative evaluations to assess the effectiveness of VIZOR in scene graph generation and downstream tasks, such as query-based object grounding. VIZOR outperforms state-of-the-art methods, showing clear improvements in scene graph generation and achieving 22% and 4.81% gains in zero-shot grounding accuracy on the Replica and Nr3D datasets, respectively. Project page: <https://vivekmadhavaram.github.io/vizor/>

1. Introduction

Scene understanding and reasoning is a crucial step for capturing the complete information about the structure of an environment, enabling a wide range of downstream

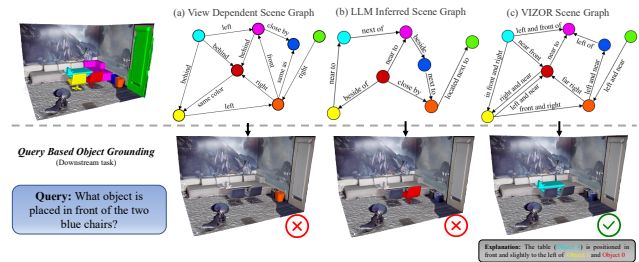


Figure 1. Overview: We present the advantage of view-invariant scene graphs generated by VIZOR, using object grounding as a downstream task. For a given complex query, view-invariant scene graphs (c) capture scene layout more accurately than (a) view-dependent scene graphs, which rely on annotator viewpoint, and (b) LLM-inferred graphs, which often produce overly generic relations.

tasks. These downstream tasks include scene captioning [14, 29, 40, 60, 72], robotic navigation [3, 5, 6, 24, 38, 43, 58], scene manipulation [10, 11, 20, 51], change detection [35], visual question answering [23, 27, 39, 41] to mention a few. An effective approach to scene understanding involves constructing a scene graph, a structured representation where objects are modeled as nodes, object features as attributes, and relationships among them as edges. An accurate scene graph enables machines to infer spatial and semantic relationships among objects, providing a strong foundation for cognitive perception in various autonomous systems.

Existing approaches [26, 34, 37, 71], for scene graph generation, predominantly rely on supervised learning, where models are trained to predict object relationships using pre-annotated ground truth datasets. However, the availability of large-scale, dense and well-annotated 3D scene graph datasets is highly limited, restricting these approaches to specific scene types and makes model training infeasible in many real-world use cases. Furthermore, datasets such as 3DSSG [55], annotate spatial and proximity relationships relative to a specific reference view, meaning relationships like “left/right” or “front” are defined based on the annotator’s perspective. An example is shown in Figure 1(a). As a result, these scene graphs become inconsistent when the

*Equal Contribution

†Current Affiliation: IBM Research India (Arkadipta.De@ibm.com)

viewpoint changes, limiting their generalization and applicability to different perspectives and practical applications.

To eliminate the dependency on annotated datasets, recent approaches (e.g., [15]) have started exploring the use of Large Language Models (LLMs) to infer object relationships based on common-sense knowledge. While LLMs can generate plausible relations, they lack scene-specific contextual grounding, often producing generic relations. For instance, consider Figure 1(b): two chairs are positioned around a table at the same distance, but their spatial positions differ. The relation inferred between the table and these chairs is “near to”. However, using only this relation for grounding one chair w.r.t the table introduces ambiguity, since both chairs satisfy the condition equally, and it’s unclear which is being referred to. Incorporating directional information like “left/right”, defined relative to each object’s front-facing direction, resolves the ambiguity.

Apart from dataset limitations, few existing methods [31] rely on a fixed coordinate system considering (x, y, z) values to define spatial relationships, which can lead to inconsistencies. Typically, one axis is assigned to determine each directional relation. For example, x-axis is used for “front/behind”, y-axis for “left/right”, and z-axis for “above/below”. However, such annotations ignore object orientation, leading to incorrect relations that fail to perform reasoning. Let us assume, for scene in Figure 1, if “front” is inferred solely based on increasing x-coordinate values, the system might incorrectly return “recycle bin” as the object in front of the chairs, simply because it has a greater x-coordinate than that of chairs. However, based on the actual orientation of the chairs, the correct answer should be “table”. This discrepancy arises because axis-based annotation does not account for object-facing direction, leading to semantically incorrect inferences.

To address all the discussed limitations, VIZOR efficiently generates 3D scene graphs, as in Figure 1(c), in a training-free manner using only the input 3D scene. At the core of our approach is a novel object-centric relational framework. VIZOR first detects objects in the scene and determines their front directions. This step is crucial because, it allows spatial relationships to be inferred *relative to how each object is oriented*, rather than relying on the *viewpoint of an annotator*. This ensures that spatial and functional relationships remain consistent regardless of observer position, a key limitation in prior works. Using the estimated front directions and object centroids, VIZOR computes bidirectional relationships between object pairs, resulting in a dense and semantically coherent scene graph. Additionally, VIZOR aggregates multi-view object renderings to extract rich object properties, such as appearance, geometry, functionality, and color. These properties are incorporated as node attributes in the graph, enhancing its expressiveness and supporting downstream tasks.

Our Contributions: To the best of our knowledge, we are the first to introduce a zero-shot method for view-independent 3D scene graph generation with relations from the object’s perspective. Our contributions are as follows: *i*) We introduce a training-free framework that constructs structured 3D scene graphs directly from scene meshes, eliminating the need for additional information like RGB-D sequences or scene graph annotated datasets. *ii*) We introduce an object-centric relation generation mechanism that models spatial relations from the intrinsic viewpoint of each object, making these relations invariant to the observer’s viewpoint. *iii*) We construct detailed 3D scene graphs where objects serve as nodes, enriched with aggregated attributes and edges represent dense open-vocabulary relations between object pairs. This enables open-ended and fine-grained reasoning over the 3D scene. *iv*) We validate the effectiveness of VIZOR through extensive qualitative and quantitative evaluations and demonstrate its utility in downstream tasks such as text-based open vocabulary object grounding using generated scene graphs.

2. Related Works

3D Scene Graph Generation: Early work introduced hierarchical structures combining buildings, rooms, objects, and cameras [4], later extended to large-scale environments [19, 45, 46]. Other methods infer local semantic inter-object relationships [25, 56, 67, 68]. Recent approaches [26, 34, 37, 71] are fully supervised, relying on annotated graphs such as 3DSSG [55]. However, these annotations are limited by their dependence on specific observer’s perspective and include sparse relations, which restricts generalization. Models trained on such data typically produce scene graphs valid only from that specific viewpoint, motivating the need for view-invariant 3D scene graph generation.

Open Vocabulary 3D Scene Graph Generation: Open-Vocabulary methods aim to infer diverse, unconstrained relations beyond fixed label sets. ConceptGraphs [15] leverages 2D vision-language-models like GPT-4 [1] and Llava [32] to build queryable 3D scene graphs with captions. However, it relies on limited frames containing a subset of objects and lacks contextual grounding, often producing generic relations disconnected from full 3D scene structure.

LLMs and VLMs for Scene Understanding: LLMs and Vision-Language Models (VLMs) have advanced instruction-driven 3D scene understanding and synthesis. InstructScene [30] combines semantic graph prior with VLM-based layout decoding for controllable synthesis, while Layout-GPT [13] composes in-context demonstrations for plausible layout generation. These methods highlight LLMs ability to capture complex scene relationships.

2D and 3D Object Grounding: Grounding localized objects in 2D or 3D data based on textual queries. One-stage methods jointly embed text and visual features for di-

rect bounding-box regression [22, 36], while two-stage approaches follow *detect-and-match* paradigm [2, 7, 63, 64], generating object proposals and then matching them to language. Graph-based methods [53, 57] infer spatial relations by connecting objects into relational graphs [2, 17, 66]. Transformer-based approaches [16, 18, 36, 44, 62] further improve grounding. Recent zero-shot method ZS3DVG [65], VLMGrounder [59] removes training via LLMs/VLMs and visual programming, but lacks global scene structure and spatial reasoning. VPP-Net [49] investigates the significance of viewpoint information and proposes uniform object representation loss to encourage viewpoint invariance in learned object representations. 3DTRL [48] proposes a token representation layer which estimates the 3D positional information of the visual tokens and leverages it for learning viewpoint-agnostic representations.

Differentiating from prior methods, we propose a training-free, viewpoint-invariant approach for generating dense and expressive 3D scene graphs. Our graphs support open-vocabulary object classes and relations and enable complex spatial and semantic reasoning for downstream tasks without relying on annotations or fixed observer viewpoints.

3. Proposed Method

This section presents our proposed method for generating 3D scene graphs. VIZOR takes a 3D scene mesh as input and generates a graph with objects in the scene as nodes and relations between them as edges. Each node in the scene graph has a set of visual and geometric attributes like color, functionality, geometry and caption. An edge between two nodes represents open-vocabulary relations.

Formally, given an input 3D scene mesh $\mathcal{S} = (\mathcal{P}, \mathcal{F})$ where $\mathcal{P} \in \mathbb{R}^{M \times 6}$ is the set of colored point cloud vertices and \mathcal{F} is the set of faces, VIZOR constructs a 3D scene graph, $\mathcal{G} = (\mathcal{V}, \mathcal{E})$ where \mathcal{V} is set of object nodes and \mathcal{E} is the set of relationships (directed edges). The set of nodes is represented as $\mathcal{V} = \{v_i \mid v_i = (o_i, c_i, A_i)\}$, where v_i represents an object node with object ID o_i , class label c_i , and a set of attributes A_i , $A_i = \{a_1, a_2, \dots, a_m\}$. The set of relationships is given by $\mathcal{E} = \{e_{ij} \mid e_{ij} = (i, j, r_{ij}, d_{ij}, \theta_{ij})\}$ where e_{ij} represents an edge from v_i to v_j with a relationship label r_{ij} , distance between centroids d_{ij} , and angle θ_{ij} , an orientation of v_i with respect to front vector of object v_j . The overall method to generate the scene graph \mathcal{G} is shown in Figure 2. It comprises of three main stages: 1) Object segmentation and finding the front direction of each object, 2) Attribute generation for each object, and 3) Predicting relations between pairs of objects.

3.1. Object Segmentation & Front Direction Estimation

To construct a view invariant 3D scene graph, we begin by identifying object instances in the scene. Our framework

supports any off-the-shelf 3D segmentation method (e.g., SAM3D [61], Mask3D [47], OpenMask3D [52]) to determine objects that serve as nodes. In our implementation, we use Mask3D for instance-level segmentation, producing segmented object meshes \mathcal{M}_i , each centered at $\mathbf{c}_{\text{obj}} \in \mathbb{R}^3$. Following segmentation, the next objective is to estimate its *front-facing direction*, which is crucial for constructing a *non observer-perspective, invariant* scene graph. Here, the relations are defined over subject-object pairs, where the subject is the entity from which the relation originates, and the object is the one to which it applies. To accurately compute these spatial relationships, both the front direction and positions of the involved entities are required.

To infer front direction, we build a reference database \mathcal{R} containing one front-view image per class across the 200 Mask3D-recognizable categories [47]. For each class, we generate a 3D object using Shap-E [21], a transformer-based generative model. Since generated object can be fully controlled, it is rotated by a fixed angle such that it faces the camera, and the resulting image is saved as class-specific front-view reference. Front views of missing objects in the reference database can be generated during inference.

Next, for a segmented object \mathcal{M}_i , we simulate a circular camera rig of radius r in the plane parallel to XY-plane, centered at object centroid $\mathbf{c}_{\text{obj}} \in \mathbb{R}^3$. A camera is moved along this rig at N uniformly spaced azimuth angles θ_k to capture multi-view renderings of the object:

$$\mathbf{c}_{\text{cam}}^{(k)} = \mathbf{c}_{\text{obj}} + r \begin{bmatrix} \cos \theta_k \\ \sin \theta_k \\ 0 \end{bmatrix}, \quad \theta_k = \frac{2\pi k}{N}, \quad k = 1, \dots, N. \quad (1)$$

The resulting multi-view images $\{I^{(k)}\}$ are compared against the class-specific reference image I_{ref} (retrieved using class label from \mathcal{R}) by a multi-modal LLM (MLLM), which is prompted to identify the front view and confidence scores of each view to I_{ref} for being the front view. The response generated by MLLM is used to retrieve best matching front view camera position. The selected camera position $\mathbf{c}_{\text{cam}}^{(k^*)}$ defines the object's front direction unit vector:

$$\hat{\mathbf{f}}_{\text{obj}} = \frac{\mathbf{c}_{\text{cam}}^{(k^*)} - \mathbf{c}_{\text{obj}}}{\|\mathbf{c}_{\text{cam}}^{(k^*)} - \mathbf{c}_{\text{obj}}\|} \quad (2)$$

Given object centroid \mathbf{c}_{obj} , we compute relative vector:

$$\mathbf{r}_{\text{obj} \rightarrow \text{cam}} = \mathbf{c}_{\text{cam}}^{(k^*)} - \mathbf{c}_{\text{obj}} \quad (3)$$

Resolving Ambiguous Front View: For symmetric objects where the front direction is ambiguous (confidence score of more than one view is greater than a front-view threshold), we resolve the ambiguity by selecting the direction that is most aligned with the center of the scene. Let $\{\mathbf{r}_{\text{obj} \rightarrow \text{cam}}^{(i)}\}$ denote the set of candidate front direction vectors for object \mathcal{M}_i , derived from multiple object-camera viewpoint configurations. We select the vector forming the

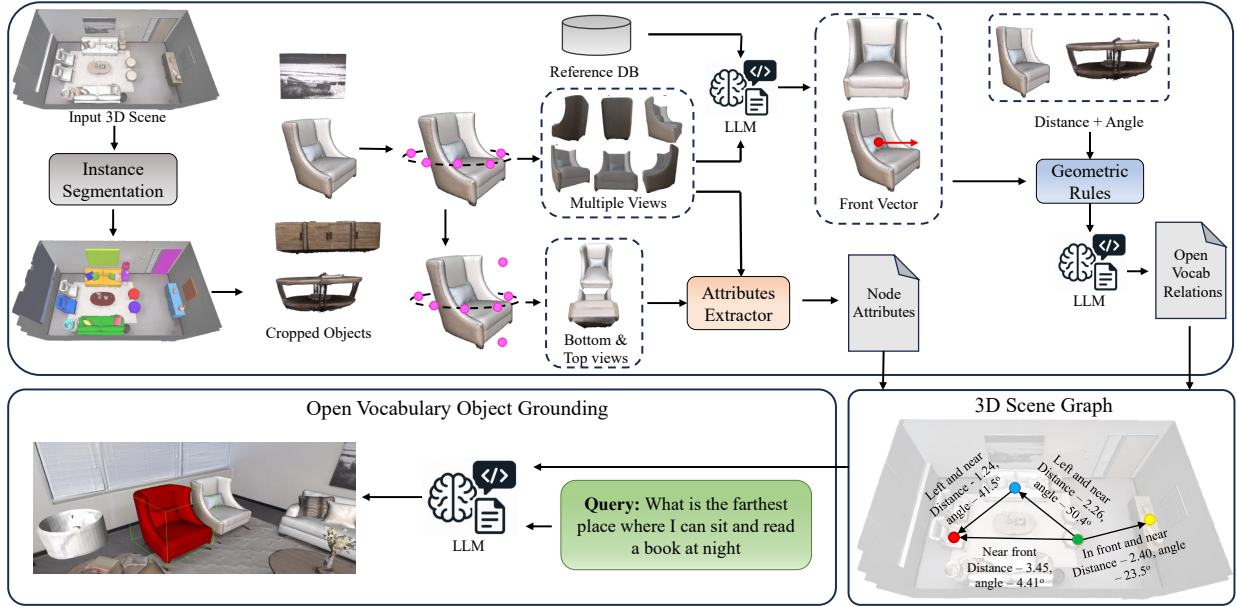


Figure 2. **Overall architecture of VIZOR.** It has three major components: Object Segmentation & Front-direction prediction module (Sec 3.1), object attribute extraction module (Sec 3.2), and Relationship extraction and enrichment module (Sec 3.3). Given only an input 3D scene mesh data, it generates a 3D view-invariant scene graph that can be directly applied to a variety of tasks *viz.* query based open vocabulary object grounding, complex scene understanding etc.

smallest angle with the vector pointing from the object centroid \mathbf{c}_{obj} to the scene center $\mathbf{c}_{\text{scene}}$:

$$\mathbf{r}_{\text{obj} \rightarrow \text{cam}} = \arg \min_i \cos^{-1} \left(\frac{\mathbf{r}_{\text{obj} \rightarrow \text{cam}}^{(i)} \cdot (\mathbf{c}_{\text{scene}} - \mathbf{c}_{\text{obj}})}{\|\mathbf{r}_{\text{obj} \rightarrow \text{cam}}^{(i)}\| \cdot \|\mathbf{c}_{\text{scene}} - \mathbf{c}_{\text{obj}}\|} \right) \quad (4)$$

3.2. Attribute Extraction for Graph Nodes

Each node in our scene graph is represented by a set of descriptive attributes obtained by Attributes Extractor from Figure 2. These attributes encapsulate various object properties, including physical characteristics (e.g., color, geometry), functionality, style, and semantic descriptions.

With segmented objects and estimated front directions available from Sec 3.1, we generate additional views to support attribute extraction. Specifically, we position a virtual camera in the object’s front direction and render a top view by moving camera along positive Z-axis in such a way that its elevation is increased and rotating it towards the object centroid. Similarly, bottom view is captured by moving camera along the negative Z axis. In addition to these, we select every alternate view from the multi-view renderings used in Sec 3.1. All of these views are passed to pre-trained MLLM, along with a structured prompt that specifies the types of attributes to extract. For each view, the model outputs a structured JSON containing various object properties, including color, geometry, functionality, structural details, and a descriptive caption. To obtain a unified representation of the object, we aggregate all per-view JSON outputs by prompting an LLM to consolidate them into a single sum-

mary JSON. This final representation captures complementary cues observed across different viewpoints.

Each node in the scene graph is thus defined by the segmented object \mathcal{M}_i and a consolidated attribute set A_i . This representation enables a richer understanding of the scene, allowing for downstream reasoning tasks such as relationship inference, object classification and grounding.

3.3. Computing Edges between Pairs of Objects

The final and most crucial step in constructing a scene graph is establishing edges, which encode the spatial and proximity relationships between subject-object pairs in the scene. Rather than relying on a fixed set of pre-defined relationships, we predict open vocabulary relationships to capture spatial relations in detailed way. Each edge represents a directed connection from a subject node to an object node, indicating spatial configuration of the subject relative to the object in scene layout.

To infer these relations, we leverage: the front direction vector of the object $\hat{\mathbf{f}}_{\text{obj}}$ (Sec 3.1), and the centroids of both the subject $\mathbf{c}_{\text{obj}_i}$ and the object $\mathbf{c}_{\text{obj}_j}$. We compute the euclidean $distance d_{ij} = \|\mathbf{c}_{\text{obj}_i} - \mathbf{c}_{\text{obj}_j}\|$ and the angle θ_{ij} between the object’s front direction $\hat{\mathbf{f}}_j$ and the vector pointing from the object to the subject, defined as $\vec{\mathbf{v}}_{ji} = \mathbf{c}_{\text{obj}_i} - \mathbf{c}_{\text{obj}_j}$. This angle captures the relative orientation of the subject with respect to the object’s viewing direction.

We define a set of geometric rules based on these features to predict the initial set of spatial relationships *viz.* “in front of”, “behind”, “left”, “right” etc. More complex spatial re-

lations like “right and above”, “left and behind”, “in front of and to the right” etc., are defined through conjunctions of geometric rules based on the angle between the centroids of the object and subject. Vertical and contact relationships like “above”, “below”, “on”, etc., are determined by analyzing bounding box extents and distance between centroids.

For each segmented object, we iteratively assign it the role of the object, and compute its relationships with all other subjects. This process continues until every segment in the scene has been treated as the object once. The result is a dense set of directed edges capturing all pairwise spatial interactions. To enhance semantic richness, the full set of predicted relationships, along with the object-level features (i.e., position, bounding box extent, and other extracted properties as described in Sec 3.2), are passed to LLM. The LLM generates open-vocabulary descriptions that combine spatial and semantic cues, including proximity terms like “near” and “far”. Detailed generation of these relations and prompts are mentioned in supplementary.

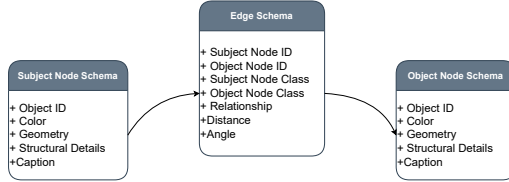


Figure 3. Scene Graph Schema

Finally, each edge in the scene graph is a tuple consisting of the subject and object information, relationship r_{ij} , distance between the pairs d_{ij} , and angle between the pairs θ_{ij} . The schema of nodes and edges are shown in Figure 3.

4. Experiments

4.1. Datasets

Replica: Replica [50] is a synthetic 3D dataset containing 18 highly photo-realistic 3D indoor scene reconstructions of rooms, offices, hotels, and apartments. Each scene includes dense mesh, high-resolution, high-dynamic-range (HDR) textures, per-primitive semantic and instance annotations, and planar mirror and glass reflectors. We use the rooms and office scenes for our experiments.

Nr3D: The Nr3D dataset [2] provides natural language referential annotations for the ScanNet 3D scene dataset [9], containing 45,503 utterances across 707 indoor scenes. Each scene includes up to six distractors (objects that belong to the same class as the target) and multiple utterances that ground an object in the scene. The utterances are categorized by difficulty (easy and hard) and by dependence on viewpoint (view-dependent and view-independent).

3DSSG: 3DSSG [55], based on 3RScan [54], contains 3D scenes annotated with over 1.6 million spatial and functional relationships represented as scene graphs, where ob-

jects are nodes and relations (spatial/semantic) are edges. In this work, we use a few randomly sampled scenes from 3DSSG for qualitative analysis to visualize and interpret our model’s predictions.

4.2. Scene Graph Construction

We evaluate scene graph construction on the Replica dataset [50], following the protocol in [15], by selecting 8 scenes (room0 to room2 and office0 to office4). Given the open-vocabulary nature of generated scene graphs and the subjectivity involved in its evaluation, we assess by involving human evaluators. 3 annotators evaluate each node and edge. We compute *node precision* as the fraction of nodes for which at least 2 of 3 human evaluators deem the node caption to be correct. Similarly, an edge (relation between object pairs) is deemed correct if 2 out of 3 evaluators agree on its validity, forming our *edge precision*. The total number of nodes for evaluation is 134, and we also report the *total number of predicted relationships* in the last column. To evaluate our *front-view prediction* (Sec 3.1), we compute the fraction of predicted-front views of segmented objects for which at least 2 out of 3 evaluators deem it to be front-view. The results are shown in Table 1.

Scene	Node Prec.			Front-View Prec.	Edge Prec.	# Edges	
	CG	CG-D	VIZOR (LLaMA)				
room0	0.78	0.56	0.71	0.91	0.67	0.66	420
room1	0.77	0.70	0.61	0.94	0.72	0.71	306
room2	0.66	0.54	0.60	1.00	0.80	0.73	210
office0	0.65	0.59	0.55	0.63	0.82	0.87	110
office1	0.65	0.49	0.58	0.83	0.75	0.71	132
office2	0.75	0.67	0.65	0.90	0.55	0.64	380
office3	0.68	0.71	0.77	0.88	0.58	0.55	272
office4	-	-	0.70	0.85	0.47	0.52	380
Average	0.71	0.61	0.65	0.88	0.65	0.67	276

Table 1. Accuracy of constructed scene graphs on Replica: Node Prec.: Accuracy of each node caption; Front-View Prec.: Accuracy of predicting the front-view of segmented object correctly, Edge Prec.: Accuracy of each estimated spatial relationship, # Edges: Number of edges or relations predicted. VIZOR indicates results for both LLaMA and GPT variants. All values are evaluated by human evaluators.

We compare our method with two variants of ConceptGraphs [15]: the original implementation (CG) and ConceptGraphs-Detector (CG-D) which integrates a RAM [69] for object identification in the image and Grounding DINO [33] for open-vocabulary object detection. As shown in Table 1, VIZOR (GPT) achieves the highest node precision with a (17% improvement) over the state-of-the-art [15]. Our method also predicts significantly more edges, demonstrating a richer graph representation.

4.3. Object Grounding based on Text Queries

We evaluate object grounding on both the Replica and Nr3D datasets. We generated scene graphs using VIZOR for Replica scenes and ScanNet scenes that are included in the test set of Nr3D. Due to the absence of ground truth,

we are not able to evaluate the accuracy of the scene graphs directly. Rather, we evaluate them using downstream tasks.

Relevant Context Filtering: For complex scenes with numerous objects, the scene graph can be very large, making direct reasoning inefficient. To address this, we introduce a *scene graph pruning mechanism* that dynamically reduces the graph size based on query relevance, ensuring efficient and focused reasoning. This is achieved by embedding both the text query and each subject, predicate, and object triplet using a sentence transformer[†]. We then compute the similarity score between the query embedding and each triplet embedding, selecting the top- K most relevant relations. In our experiments, we set $K = 1500$, meaning we retrieve up to 1500 relations per query, however, in some cases, fewer relations may be selected when the number of relations are already low. It is to be noted that, we only prune the relationships and pass all the nodes along with their attributes as context to the LLM for querying.

Query Type	# Queries	CG-CLIP [15]	CG-LLM [15]	VIZOR-LLaMA	VIZOR-GPT
Descriptive	20	0.59	0.61	0.75	0.63
Affordance	5	0.43	0.57	0.8	0.8
Negation	5	0.26	0.80	0.9	1
Complex-Spatial	30	0.20	0.28	0.58	0.67
Overall	60	0.37	0.56	0.76	0.78

Table 2. Comparison of Open Vocabulary Object Grounding from Text Queries on Replica (room0 and office0): We measure the top-1 recall. CG-CLIP refers to Conceptgraph with CLIP-based retrieval using cosine similarity. CG-LLM refers to Conceptgraph with an LLM that parses the scene graph and returns the most relevant object. VIZOR always uses LLM-based retrieval techniques, and here we assess different LLMs. All values are evaluated by human evaluators.

Experimental Result on Replica: Following [15], we evaluate grounding on 2 scenes (room0, office0) from Replica. Since no ground truth is available, we employ 3 human evaluators to assess the retrieved objects and compare the results. [15] created questions on room0 and office0 scenes and categorized them in 3 types: Descriptive (e.g., “A brown chair”), Affordance (e.g., “Something to sit down”) and Negation (e.g., “place to sit but not lie down”). While [15] uses both CLIP and LLM(GPT4o)-based retrieval (CLIP selects the object with the highest similarity to the query’s embedding, LLM goes through the scene graph nodes to identify the object with the most relevant caption), we use only LLM-based retrieval where we provide the pruned scene graph as context to LLM. Table 2 shows that both VIZOR-LLaMA and VIZOR-GPT outperform [15], with VIZOR-GPT achieving a 22% improvement in overall grounding accuracy. Complex-spatial queries are discussed in Section 4.4.

Experimental Result on Nr3D: To show the generalization, we perform object grounding experiments on Nr3D

[†]<https://huggingface.co/sentence-transformers/all-mpnet-base-v2>

dataset and compare our method against fully supervised [2, 7, 8, 36, 66, 70], and state-of-the-art zero-shot methods ZS-3DVG [65], SeeGround [28], VLM-Grounder [59]. Following ZS-3DVG [65], we use ground-truth object proposals (i.e., we directly use instance segments as nodes and build scene graph by generating node attributes and relationships). We compare VIZOR with all state-of-the-art methods on the Nr3D dataset in Table 3. Our training-free model performs better or have comparable performance to supervised methods. Also, VIZOR outperforms the state-of-the-art zero-shot methods with a 4.81% overall improvement. Exciting results on Nr3D provide evidence that the performance of our model is not only restricted to one dataset but spans across different benchmark datasets.

Method	Type	Nr3D			
		Overall	Easy	Hard	View Dep
ReferIt3D [2]	Supervised	35.6	43.6	27.9	32.5
ScanRefer [7]		34.2	41.0	23.5	29.9
TGNN [17]		37.3	44.2	30.6	35.8
InstanceRefer [66]		38.8	46.0	31.8	43.5
3DVG-Trans [70]		40.8	48.5	34.8	44.3
TransRefer3D [16]		42.1	48.5	36.0	45.4
LanguageRefer [44]		43.9	51.0	36.6	47.7
SAT [62]		49.2	56.3	42.4	54.0
3D-SPS [36]		51.5	58.1	45.1	55.4
ViL3DRel [8]		64.4	70.2	57.4	62.0
ZS-3DVG [65]	Zero-shot	39.0	46.5	31.7	36.8
SeeGround [28]		46.1	54.8	38.3	42.3
VLM-Grounder [59]		48.0	55.2	39.5	45.8
VIZOR-GPT (Ours)		52.81	62.52	43.48	43.02
					57.66

Table 3. Comparison of SoTA method on Grounding Accuracy (%) on Nr3D dataset with ground-truth object proposals.

A detailed comparative discussion of different zero-shot methods including VIZOR is available in supplementary.

4.4. Complex Visual-Language Queries

While the previous methods are evaluated on object grounding based on text queries, we extend this evaluation further. For room0 and office0 scenes from Replica, we carefully construct complex visual-language queries that require spatial understanding of the scene and additional reasoning to retrieve the object from the scene. We create 30 questions per scene. A list of all the questions can be found in the supplementary. Example includes: “Where can I sit so that I can read a book at night and I want to face the cabinet while sitting?”, “What is to the 45 degree left side of the screens?”. Table 2 (4th row) compares our method with CG-CLIP and CG-LLM. Despite CG-LLM also using GPT-4o, VIZOR-GPT achieves a 39% improvement, demonstrating superior scene understanding and reasoning via structured graphs and attribute-rich nodes.

4.5. Qualitative Analysis

Analysis on Replica: We qualitatively compare VIZOR with ConceptGraphs [15] on the task of open vocabulary object grounding using complex natural language queries.

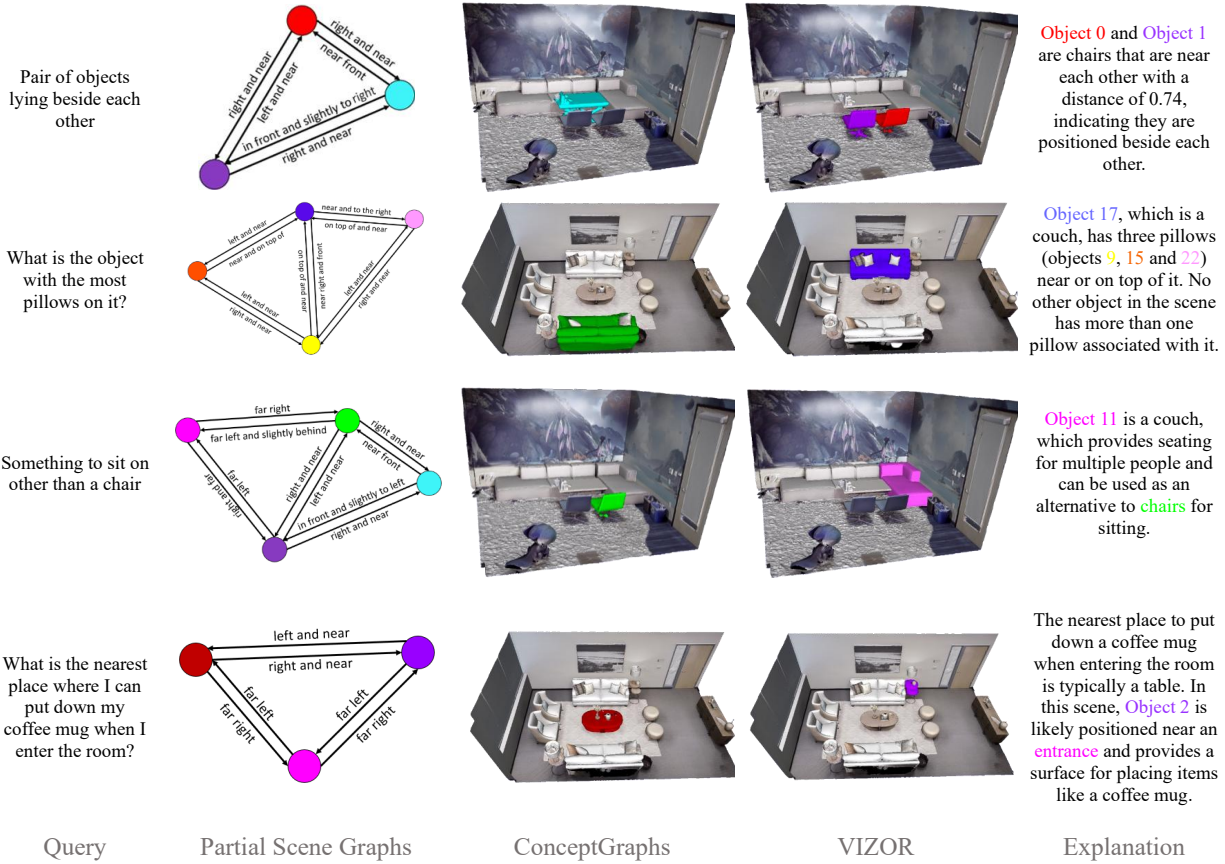


Figure 4. **Qualitative Results:** (a) Input query, (b) Part of scene graph generated by VIZOR, (c) ConceptGraphs [15], (d) VIZOR output, (e) Explanation of object grounding using VIZOR.

Figure 4 shows results for 4 queries selected from Sec 4.4. For analysis purposes, we show partial 3D scene graph generated by VIZOR in 2nd column. This graph contains the color-coded nodes required to answer the given query, along with relations between them. We observe that [15] fails in answering complex queries (3rd column). Since Concept-Graphs uses CLIP [42] similarity score to answer the query, it directly responds with the object mentioned in the query instead of understanding the semantics (Row 3). In contrast, VIZOR correctly recognizes objects even with complex queries, which is visible in the 4th column. An explanation for object grounding by VIZOR is displayed in the last column. It is also noted that, based on the query, VIZOR can refer to multiple objects as per requirement (Row 1). These results indicate that VIZOR is capable of grounding objects by understanding the semantics of the input query and input scene. More examples, along with scene graphs on ScanNet [9], are shown in supplementary.

Analysis on 3DSSG: We evaluate quality of scene graphs generated by VIZOR on 3DSSG dataset [55], comparing them against ground truth annotations (Fig. 5). We present two different scenes from 3DSSG, along with (a) ground truth 3DSSG scene graph and (b) scene graph by VIZOR. We show partial scene graphs for ease of under-

standing. The nodes are color-coded with same color as the objects, as in the input scenes. In both examples, we see more spatially accurate relationships provided by VIZOR instead of scene graphs that were annotated from a specific viewpoint in the ground truth. We also see missing relationships in ground truth (marked with red dotted line). However, VIZOR-generated graphs provide complete and spatially consistent set of relationships. We show more scene graphs on 3DSSG using VIZOR in supplementary.

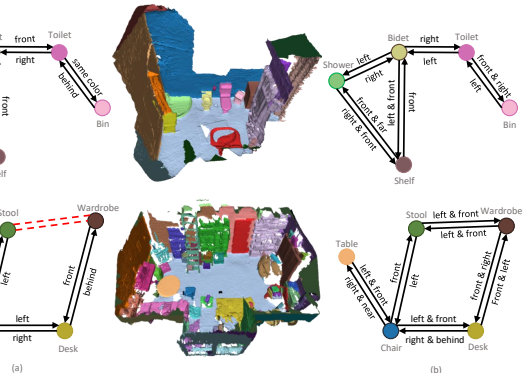


Figure 5. Comparative Scene Graph Results: Scene graph comparison between (a) 3DSSG ground truth scene graphs and (b) VIZOR generated scene graphs on 3DSSG scenes

4.6. Design Choice Analysis

We further analyze the impact of key architectural choices in VIZOR.

Front Direction Estimation: To evaluate front-direction prediction, we compare several strategies: ViT-based cosine similarity, Direct query with MLLMs without reference front-view images, and LLMs with diffusion-generated views as reference images. As shown in Table 4, our method achieves the highest front-view precision.

Method	Diffusion	Reference	Front View Precision (%)
ViT-based cosine similarity	✗	✓	82.35
Direct multimodal-LLM Query	✗	✗	80.22
LLM + 2D diffusion reference View	✓	✗	58.82
VIZOR	✗	✓	85.71

Table 4. Comparison of front-direction inference methods.

Number of Views Used: We also vary number of rendered viewpoints used for front-view prediction and observe trade-off between front view precision, token cost, and runtime (Table 5). We select balanced configuration that ensures both efficiency and performance. We randomly choose 38 objects from room0 and office0 of Replica [50] and perform the experiments on front direction design choice analysis (Table 4 and 5).

# Views	Front View Precision (%)	Avg Time (Sec.)	Avg Tokens
8	82.36	4.02	1045
12	85.71	6.67	1387
16	86.24	10.03	1726
20	86.92	14.21	2081

Table 5. Effect of number of viewpoints on Front-View Detection

Attribute Extractor: We evaluate node attribute quality across four VIZOR variants. We ask three evaluators to rate the attributes on a 1–5 Likert scale (1=“Poor”, 5=“Excellent”). The details are provided in supplementary. We test two MLLMs for attribute extraction: Llama 3.2 11B Vision-Instruct [12] and GPT4-o [1]. These variants are denoted as VIZOR-LLaMA and VIZOR-GPT. We evaluate both under two settings: attribute extraction using only the front-view (Single-View) or aggregating attributes from multiple viewpoints (Multi-View) as described in Sec 3.2. Table 6 shows that VIZOR-GPT with Multi-View aggregation achieves the highest ratings for both color and geometry extraction, and is thus used in all subsequent experiments.

5. Failure Analysis

After thorough experimentation, it is evident that VIZOR can outperform the state-of-the-art methods. Still, there is scope for improvement in the accuracy of our model. We performed extensive analysis on failure cases to understand the bottlenecks of our method in predicting the relations. Our findings are represented in Figure 6.

For this failure analysis, we considered four scenes from Replica and four scenes from the Nr3D datasets, comprising a total of 1,645 relations. We conducted a human evaluation

Scene	VIZOR-LLaMA		VIZOR-GPT		VIZOR-GPT	
	Single View	Multi View	Single View	Multi View	Single View	Multi View
room0	3.68	2.39	3.44	2.11	3.39	3.47
room1	3.69	2.42	3.23	2.57	4	4.42
room2	3.75	2.5	3.85	2.6	3.9	3.65
office0	4.07	2.07	3.93	2.29	3.93	4
office1	2.3	1.6	4	1.5	3.2	3.7
office2	4.03	2.41	3.53	2.5	4.03	4.34
office3	3.5	2.19	3.75	2.31	3.94	4.69
office4	3.95	2.59	3.69	2.38	4.18	4.10
Average	3.62	2.27	3.68	2.28	3.82	4.05
					3.86	4.25

Table 6. Rating of Node Attribute on Replica: Color refers to the color of the object and Geometry refers to the geometric appearance of the object. **Blue** refers to best performance in color and **Black** refers to best performance in geometry.

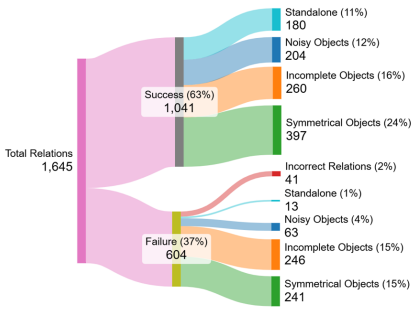


Figure 6. **Failure cases:** A graphical representation of failure cases in a hierarchical structure.

to assess the accuracy of these relations. The method can predict the correct relations in case of many symmetrical, noisy, and incomplete objects, but still fails to predict accurate relations for some symmetrical and incomplete objects. The failure of symmetrical objects is due to multiple possible front views that are at equal distance from the scene center, and our model chooses one of them, which may not be the best front view of that object. We observe a failure rate of 37% (241 out of 638 cases consisting of symmetrical objects) when employing our method (Sec 3.1). Similarly, the multi-modal LLM fails to recognize the front view of incomplete objects as it is unable to predict the geometry of that object. The failure rate is very less for standalone relations and noisy objects. Detailed failure analysis and limitations are explained in the supplementary.

6. Conclusion

We introduce VIZOR, a training-free method for generating view-invariant scene graphs for 3D scene reasoning. Given a 3D input scene, VIZOR can generate a scene graph containing detailed relations between objects. To the best of our knowledge, we are the first ones to propose a zero-shot approach for scene graph generation based on objects’ perspective. We compare our proposed method with existing approaches using qualitative, and quantitative metrics and showcase the proficiency of our method over others.

Acknowledgments: This work is supported by Fujitsu Research India Private Limited. We thank the evaluators for participating in user study evaluation.

References

[1] Josh Achiam, Steven Adler, Sandhini Agarwal, Lama Ahmad, Ilge Akkaya, Florencia Leoni Aleman, Diogo Almeida, Janko Altenschmidt, Sam Altman, Shyamal Anadkat, et al. Gpt-4 technical report. *arXiv preprint arXiv:2303.08774*, 2023. 2, 8

[2] Panos Achlioptas, Ahmed Abdelreheem, Fei Xia, Mohamed Elhoseiny, and Leonidas Guibas. Referit3d: Neural listeners for fine-grained 3d object identification in real-world scenes. In *Computer Vision–ECCV 2020: 16th European Conference, Glasgow, UK, August 23–28, 2020, Proceedings, Part I 16*, pages 422–440. Springer, 2020. 3, 5, 6

[3] Christopher Agia, Krishna Murthy Jatavallabhula, Mohamed Khodeir, Ondrej Miksik, Vibhav Vineet, Mustafa Mukadam, Liam Paull, and Florian Shkurti. Taskography: Evaluating robot task planning over large 3d scene graphs. In *Conference on Robot Learning*, pages 46–58. PMLR, 2022. 1

[4] Iro Armeni, Zhi-Yang He, JunYoung Gwak, Amir R Zamir, Martin Fischer, Jitendra Malik, and Silvio Savarese. 3d scene graph: A structure for unified semantics, 3d space, and camera. In *Proceedings of the IEEE/CVF international conference on computer vision*, pages 5664–5673, 2019. 2

[5] Hriday Bavle, Jose Luis Sanchez-Lopez, Muhammad Shah-eer, Javier Civera, and Holger Voos. Situational graphs for robot navigation in structured indoor environments. *IEEE Robotics and Automation Letters*, 7(4):9107–9114, 2022. 1

[6] Sebastian Blumenthal, Herman Bruyninckx, Walter Nowak, and Erwin Prassler. A scene graph based shared 3d world model for robotic applications. In *2013 IEEE International Conference on Robotics and Automation*, pages 453–460, 2013. 1

[7] Dave Zhenyu Chen, Angel X Chang, and Matthias Nießner. Scanrefer: 3d object localization in rgb-d scans using natural language. In *European conference on computer vision*, pages 202–221. Springer, 2020. 3, 6

[8] Shizhe Chen, Pierre-Louis Guhur, Makarand Tapaswi, Cordelia Schmid, and Ivan Laptev. Language conditioned spatial relation reasoning for 3d object grounding. *Advances in neural information processing systems*, 35:20522–20535, 2022. 6

[9] Angela Dai, Angel X Chang, Manolis Savva, Maciej Halber, Thomas Funkhouser, and Matthias Nießner. Scannet: Richly-annotated 3d reconstructions of indoor scenes. In *Proceedings of the IEEE conference on computer vision and pattern recognition*, pages 5828–5839, 2017. 5, 7

[10] Helisa Dhamo, Azade Farshad, Iro Laina, Nassir Navab, Gregory D. Hager, Federico Tombari, and Christian Rupprecht. Semantic image manipulation using scene graphs. In *Proceedings of the IEEE/CVF Conference on Computer Vision and Pattern Recognition (CVPR)*, June 2020. 1

[11] Helisa Dhamo, Fabian Manhardt, Nassir Navab, and Federico Tombari. Graph-to-3d: End-to-end generation and manipulation of 3d scenes using scene graphs. In *Proceedings of the IEEE/CVF International Conference on Computer Vision (ICCV)*, pages 16352–16361, October 2021. 1

[12] Abhimanyu Dubey, Abhinav Jauhri, Abhinav Pandey, Abhishek Kadian, Ahmad Al-Dahle, Aiesha Letman, Akhil Mathur, Alan Schelten, Amy Yang, Angela Fan, et al. The llama 3 herd of models. *arXiv preprint arXiv:2407.21783*, 2024. 8

[13] Weixi Feng, Wanrong Zhu, Tsu-jui Fu, Varun Jampani, Arjun Akula, Xuehai He, Sugato Basu, Xin Eric Wang, and William Yang Wang. Layoutgpt: Compositional visual planning and generation with large language models. *Advances in Neural Information Processing Systems*, 36:18225–18250, 2023. 2

[14] Jiaxiang Gu, Shafiq Joty, Jianfei Cai, Handong Zhao, Xu Yang, and Gang Wang. Unpaired image captioning via scene graph alignments. In *Proceedings of the IEEE/CVF International Conference on Computer Vision (ICCV)*, October 2019. 1

[15] Qiao Gu, Ali Kuwajerwala, Sacha Morin, Krishna Murthy Jatavallabhula, Bipasha Sen, Aditya Agarwal, Corban Rivera, William Paul, Kirsty Ellis, Rama Chellappa, et al. Conceptgraphs: Open-vocabulary 3d scene graphs for perception and planning. In *2024 IEEE International Conference on Robotics and Automation (ICRA)*, pages 5021–5028. IEEE, 2024. 2, 5, 6, 7

[16] Dailan He, Yusheng Zhao, Junyu Luo, Tianrui Hui, Shaofei Huang, Aixi Zhang, and Si Liu. Transrefer3d: Entity-and-relation aware transformer for fine-grained 3d visual grounding. In *Proceedings of the 29th ACM International Conference on Multimedia*, pages 2344–2352, 2021. 3, 6

[17] Pin-Hao Huang, Han-Hung Lee, Hwann-Tzong Chen, and Tyng-Luh Liu. Text-guided graph neural networks for referring 3d instance segmentation. In *Proceedings of the AAAI Conference on Artificial Intelligence*, volume 35, pages 1610–1618, 2021. 3, 6

[18] Shijia Huang, Yilun Chen, Jiaya Jia, and Liwei Wang. Multi-view transformer for 3d visual grounding. In *Proceedings of the IEEE/CVF Conference on Computer Vision and Pattern Recognition*, pages 15524–15533, 2022. 3

[19] Nathan Hughes, Yun Chang, and Luca Carlone. Hydra: A real-time spatial perception engine for 3d scene graph construction and optimization. *CoRR*, 2022. 2

[20] Ziyuan Jiao, Yida Niu, Zeyu Zhang, Song-Chun Zhu, Yixin Zhu, and Hangxin Liu. Sequential manipulation planning on scene graph. In *2022 IEEE/RSJ International Conference on Intelligent Robots and Systems (IROS)*, pages 8203–8210, 2022. 1

[21] Heewoo Jun and Alex Nichol. Shap-e: Generating conditional 3d implicit functions. *arXiv preprint arXiv:2305.02463*, 2023. 3

[22] Aishwarya Kamath, Mannat Singh, Yann LeCun, Gabriel Synnaeve, Ishan Misra, and Nicolas Carion. Mdetr-modulated detection for end-to-end multi-modal understanding. In *Proceedings of the IEEE/CVF international conference on computer vision*, pages 1780–1790, 2021. 3

[23] Franklin Kenghagho Kenfack, Feroz Ahmed Siddiqy, Ferenc Balint-Benczedi, and Michael Beetz. Robotvqa—a scene-graph-and deep-learning-based visual question answering system for robot manipulation. In *2020 IEEE/RSJ International Conference on Intelligent Robots and Systems (IROS)*, pages 9667–9674. IEEE, 2020. 1

[24] Dohyun Kim, Jinwoo Kim, Minwoo Cho, and Daehyung Park. Natural language-guided semantic navigation using scene graph. In *International Conference on Robot Intelligence Technology and Applications*, pages 148–156. Springer, 2022. 1

[25] Sebastian Koch, Pedro Hermosilla, Narunas Vaskevicius, Mirco Colosi, and Timo Ropinski. Lang3dsg: Language-based contrastive pre-training for 3d scene graph prediction. In *2024 International Conference on 3D Vision (3DV)*, pages 1037–1047. IEEE, 2024. 2

[26] Sebastian Koch, Narunas Vaskevicius, Mirco Colosi, Pedro Hermosilla, and Timo Ropinski. Open3dsg: Open-vocabulary 3d scene graphs from point clouds with queryable objects and open-set relationships. In *Proceedings of the IEEE/CVF Conference on Computer Vision and Pattern Recognition*, pages 14183–14193, 2024. 1, 2

[27] Soohyeong Lee, Ju-Whan Kim, Youngmin Oh, and Joo Hyuk Jeon. Visual question answering over scene graph. In *2019 First International Conference on Graph Computing (GC)*, pages 45–50. IEEE, 2019. 1

[28] Rong Li, Shijie Li, Lingdong Kong, Xulei Yang, and Junwei Liang. Seleground: See and ground for zero-shot open-vocabulary 3d visual grounding. In *Proceedings of the Computer Vision and Pattern Recognition Conference (CVPR)*, pages 3707–3717, June 2025. 6

[29] Xiangyang Li and Shuqiang Jiang. Know more say less: Image captioning based on scene graphs. *IEEE Transactions on Multimedia*, 21(8):2117–2130, 2019. 1

[30] Chenguo Lin and MU Yadong. Instructscene: Instruction-driven 3d indoor scene synthesis with semantic graph prior. In *The Twelfth International Conference on Learning Representations*, 2023. 2

[31] Sergey Linok, Tatiana Zemskova, Svetlana Ladanova, Roman Titkov, Dmitry Yudin, Maxim Monastyrny, and Aleksei Valenkov. Beyond bare queries: Open-vocabulary object grounding with 3d scene graph, 2024. 2

[32] Haotian Liu, Chunyuan Li, Qingyang Wu, and Yong Jae Lee. Visual instruction tuning. *Advances in neural information processing systems*, 36:34892–34916, 2023. 2

[33] Shilong Liu, Zhaoyang Zeng, Tianhe Ren, Feng Li, Hao Zhang, Jie Yang, Qing Jiang, Chunyuan Li, Jianwei Yang, Hang Su, et al. Grounding dino: Marrying dino with grounded pre-training for open-set object detection. In *European Conference on Computer Vision*, pages 38–55. Springer, 2024. 5

[34] Yuanyuan Liu, Chengjiang Long, Zhaoxuan Zhang, Bokai Liu, Qiang Zhang, Baocai Yin, and Xin Yang. Explore contextual information for 3d scene graph generation. *IEEE Transactions on Visualization and Computer Graphics*, 29(12):5556–5568, 2022. 1, 2

[35] Samuel Looper, Javier Rodriguez-Puigvert, Roland Siegwart, Cesar Cadena, and Lukas Schmid. 3d vsg: Long-term semantic scene change prediction through 3d variable scene graphs. In *2023 IEEE International Conference on Robotics and Automation (ICRA)*, pages 8179–8186. IEEE, 2023. 1

[36] Junyu Luo, Jiahui Fu, Xianghao Kong, Chen Gao, Haibing Ren, Hao Shen, Huaxia Xia, and Si Liu. 3d-sps: Single-stage 3d visual grounding via referred point progressive selection. In *Proceedings of the IEEE/CVF Conference on Computer Vision and Pattern Recognition*, pages 16454–16463, 2022. 3, 6

[37] Changsheng Lv, Mengshi Qi, Xia Li, Zhengyuan Yang, and Huadong Ma. Sgformer: Semantic graph transformer for point cloud-based 3d scene graph generation. In *Proceedings of the AAAI Conference on Artificial Intelligence*, volume 38, pages 4035–4043, 2024. 1, 2

[38] Zhe Ni, Xiaoxin Deng, Cong Tai, Xinyue Zhu, Qinghongbing Xie, Weihang Huang, Xiang Wu, and Long Zeng. Grid: Scene-graph-based instruction-driven robotic task planning. In *2024 IEEE/RSJ International Conference on Intelligent Robots and Systems (IROS)*, pages 13765–13772, 2024. 1

[39] Sai Vidyaranya Nuthalapati, Ramraj Chandradevan, Eleonora Giunchiglia, Bowen Li, Maxime Kayser, Thomas Lukasiewicz, and Carl Yang. Lightweight visual question answering using scene graphs. In *Proceedings of the 30th ACM International Conference on Information & Knowledge Management*, pages 3353–3357, 2021. 1

[40] Itthisak Phueaksri, Marc A. Kastner, Yasutomo Kawanishi, Takahiro Komamizu, and Ichiro Ide. An approach to generate a caption for an image collection using scene graph generation. *IEEE Access*, 11:128245–128260, 2023. 1

[41] Tianwen Qian, Jingjing Chen, Shaoxiang Chen, Bo Wu, and Yu-Gang Jiang. Scene graph refinement network for visual question answering. *IEEE Transactions on Multimedia*, 25:3950–3961, 2022. 1

[42] Alec Radford, Jong Wook Kim, Chris Hallacy, Aditya Ramesh, Gabriel Goh, Sandhini Agarwal, Girish Sastry, Amanda Askell, Pamela Mishkin, Jack Clark, et al. Learning transferable visual models from natural language supervision. In *International conference on machine learning*, pages 8748–8763. PMLR, 2021. 7

[43] Krishan Rana, Jesse Haviland, Sourav Garg, Jad Abou-Chakra, Ian Reid, and Niko Suenderhauf. Sayplan: Grounding large language models using 3d scene graphs for scalable robot task planning. *arXiv preprint arXiv:2307.06135*, 2023. 1

[44] Junha Roh, Karthik Desingh, Ali Farhadi, and Dieter Fox. Languageref: Spatial-language model for 3d visual grounding. In *Conference on Robot Learning*, pages 1046–1056. PMLR, 2022. 3, 6

[45] Antoni Rosinol, Arjun Gupta, Marcus Abate, Jingnan Shi, and Luca Carlone. 3d dynamic scene graphs: Actionable spatial perception with places, objects, and humans. In *Robotics: Science and Systems*, 2020. 2

[46] Antoni Rosinol, Andrew Violette, Marcus Abate, Nathan Hughes, Yun Chang, Jingnan Shi, Arjun Gupta, and Luca Carlone. Kimera: From slam to spatial perception with 3d dynamic scene graphs. *The International Journal of Robotics Research*, 40(12-14):1510–1546, 2021. 2

[47] Jonas Schult, Francis Engelmann, Alexander Hermans, Or Litany, Siyu Tang, and Bastian Leibe. Mask3d: Mask transformer for 3d semantic instance segmentation. In *2023 IEEE International Conference on Robotics and Automation (ICRA)*, pages 8216–8223, 2023. 3

[48] Jinghuan Shang, Srijan Das, and Michael Ryoo. Learning viewpoint-agnostic visual representations by recovering tokens in 3d space. *Advances in Neural Information Processing Systems*, 35:31031–31044, 2022. 3

[49] Xiangxi Shi, Zhonghua Wu, and Stefan Lee. Viewpoint-aware visual grounding in 3d scenes. In *2024 IEEE/CVF Conference on Computer Vision and Pattern Recognition (CVPR)*, pages 14056–14065, 2024. 3

[50] Julian Straub, Thomas Whelan, Lingni Ma, Yufan Chen, Erik Wijmans, Simon Green, Jakob J. Engel, Raul Mur-Artal, Carl Ren, Shobhit Verma, Anton Clarkson, Mingfei Yan, Brian Budge, Yajie Yan, Xiaqing Pan, June Yon, Yuyang Zou, Kimberly Leon, Nigel Carter, Jesus Brailes, Tyler Gillingham, Elias Mueggler, Luis Pesqueira, Manolis Savva, Dhruv Batra, Hauke M. Strasdat, Renzo De Nardi, Michael Goesele, Steven Lovegrove, and Richard Newcombe. The Replica dataset: A digital replica of indoor spaces. *arXiv preprint arXiv:1906.05797*, 2019. 5, 8

[51] Sitong Su, Lianli Gao, Junchen Zhu, Jie Shao, and Jingkuan Song. Fully functional image manipulation using scene graphs in a bounding-box free way. In *Proceedings of the 29th ACM International Conference on Multimedia, MM '21*, page 1784–1792, New York, NY, USA, 2021. Association for Computing Machinery. 1

[52] Ayça Takmaz, Elisabetta Fedele, Robert Sumner, Marc Pollefeys, Federico Tombari, and Francis Engelmann. Open-mask3d: Open-vocabulary 3d instance segmentation. In *Thirty-seventh Conference on Neural Information Processing Systems*, 2023. 3

[53] Petar Veličković, Guillem Cucurull, Arantxa Casanova, Adriana Romero, Pietro Liò, and Yoshua Bengio. Graph attention networks. In *International Conference on Learning Representations*, 2018. 3

[54] Johannes Wald, Markus Dahnert, Daniel Rückert, Manolis Savva, Carsten Rother, Federico Tombari, and Nassir Navab. 3rscan: A reality-based 3d dataset for scene understanding. In *Proceedings of the IEEE/CVF Conference on Computer Vision and Pattern Recognition (CVPR)*, pages 8180–8189, 2020. 5

[55] Johanna Wald, Helisa Dhamo, Nassir Navab, and Federico Tombari. Learning 3d semantic scene graphs from 3d indoor reconstructions. In *Conference on Computer Vision and Pattern Recognition (CVPR)*, 2020. 1, 2, 5, 7

[56] Johanna Wald, Helisa Dhamo, Nassir Navab, and Federico Tombari. Learning 3d semantic scene graphs from 3d indoor reconstructions. In *Proceedings of the IEEE/CVF Conference on Computer Vision and Pattern Recognition*, pages 3961–3970, 2020. 2

[57] Yue Wang, Yongbin Sun, Ziwei Liu, Sanjay E Sarma, Michael M Bronstein, and Justin M Solomon. Dynamic graph cnn for learning on point clouds. *ACM Transactions on Graphics (tog)*, 38(5):1–12, 2019. 3

[58] Abdelrhman Werby, Chenguang Huang, Martin Büchner, Abhinav Valada, and Wolfram Burgard. Hierarchical open-vocabulary 3d scene graphs for language-grounded robot navigation. In *First Workshop on Vision-Language Models for Navigation and Manipulation at ICRA 2024*, 2024. 1

[59] Runsen Xu, Zhiwei Huang, Tai Wang, Yilun Chen, Jiangmiao Pang, and Dahua Lin. Vlm-grounder: A vlm agent for zero-shot 3d visual grounding. In *8th Annual Conference on Robot Learning*, 2024. 3, 6

[60] Xu Yang, Kaihua Tang, Hanwang Zhang, and Jianfei Cai. Auto-encoding scene graphs for image captioning. In *Proceedings of the IEEE/CVF Conference on Computer Vision and Pattern Recognition (CVPR)*, June 2019. 1

[61] Yunhan Yang, Xiaoyang Wu, Tong He, Hengshuang Zhao, and Xihui Liu. Sam3d: Segment anything in 3d scenes. *arXiv preprint arXiv:2306.03908*, 2023. 3

[62] Zhengyuan Yang, Songyang Zhang, Liwei Wang, and Jiebo Luo. Sat: 2d semantics assisted training for 3d visual grounding. In *Proceedings of the IEEE/CVF International Conference on Computer Vision*, pages 1856–1866, 2021. 3, 6

[63] Licheng Yu, Zhe Lin, Xiaohui Shen, Jimei Yang, Xin Lu, Mohit Bansal, and Tamara L Berg. Mattnet: Modular attention network for referring expression comprehension. In *Proceedings of the IEEE conference on computer vision and pattern recognition*, pages 1307–1315, 2018. 3

[64] Licheng Yu, Patrick Poirson, Shan Yang, Alexander C Berg, and Tamara L Berg. Modeling context in referring expressions. In *Computer Vision–ECCV 2016: 14th European Conference, Amsterdam, The Netherlands, October 11–14, 2016, Proceedings, Part II 14*, pages 69–85. Springer, 2016. 3

[65] Zhihao Yuan, Jinke Ren, Chun-Mei Feng, Hengshuang Zhao, Shuguang Cui, and Zhen Li. Visual programming for zero-shot open-vocabulary 3d visual grounding. In *Proceedings of the IEEE/CVF Conference on Computer Vision and Pattern Recognition*, pages 20623–20633, 2024. 3, 6

[66] Zhihao Yuan, Xu Yan, Yinghong Liao, Ruimao Zhang, Sheng Wang, Zhen Li, and Shuguang Cui. Instancerefer: Cooperative holistic understanding for visual grounding on point clouds through instance multi-level contextual referring. In *Proceedings of the IEEE/CVF International Conference on Computer Vision*, pages 1791–1800, 2021. 3, 6

[67] Chaoyi Zhang, Jianhui Yu, Yang Song, and Weidong Cai. Exploiting edge-oriented reasoning for 3d point-based scene graph analysis. In *Proceedings of the IEEE/CVF conference on computer vision and pattern recognition*, pages 9705–9715, 2021. 2

[68] Shoulong Zhang, Aimin Hao, Hong Qin, et al. Knowledge-inspired 3d scene graph prediction in point cloud. *Advances in Neural Information Processing Systems*, 34:18620–18632, 2021. 2

[69] Youcai Zhang, Xinyu Huang, Jinyu Ma, Zhaoyang Li, Zhaochuan Luo, Yanchun Xie, Yuzhuo Qin, Tong Luo, Yaqian Li, Shilong Liu, et al. Recognize anything: A strong image tagging model. In *Proceedings of the IEEE/CVF Conference on Computer Vision and Pattern Recognition*, pages 1724–1732, 2024. 5

[70] Lichen Zhao, Daigang Cai, Lu Sheng, and Dong Xu. 3dvg-transformer: Relation modeling for visual grounding on point clouds. In *Proceedings of the IEEE/CVF International Conference on Computer Vision*, pages 2928–2937, 2021. 6

- [71] Yiwu Zhong, Jing Shi, Jianwei Yang, Chenliang Xu, and Yin Li. Learning to generate scene graph from natural language supervision. In *Proceedings of the IEEE/CVF International Conference on Computer Vision*, pages 1823–1834, 2021. [1](#), [2](#)
- [72] Yiwu Zhong, Liwei Wang, Jianshu Chen, Dong Yu, and Yin Li. Comprehensive image captioning via scene graph decomposition. In Andrea Vedaldi, Horst Bischof, Thomas Brox, and Jan-Michael Frahm, editors, *Computer Vision – ECCV 2020*, pages 211–229, Cham, 2020. Springer International Publishing. [1](#)